Universiteit Antwerpen

This item is the archived peer-reviewed author-version of:

Aligning graphene in bulk copper : nacre-inspired nanolaminated architecture coupled with in-situ processing for enhanced mechanical properties and high electrical conductivity

Reference:
Cao Mu, Xiong Ding-Bang, Tan Zhanqiu, Ji Gang, Amin-Ahmadi Behnam, Guo Qiang, Fan Genlian, Guo Cuiping, Li Zhiqiang, Zhang Di.- Aligning graphene in bulk copper : nacre-inspired nanolaminated architecture coupled w ith in-situ processing for enhanced mechanical properties and high electrical conductivity
Carbon - ISSN 0008-6223 - 117(2017), p. 65-74
Full text (Publisher's DOI): https://doi.org/10.1016/J.CARBON.2017.02.089

uantwerpen.be
Institutional repository IRUA

Accepted Manuscript

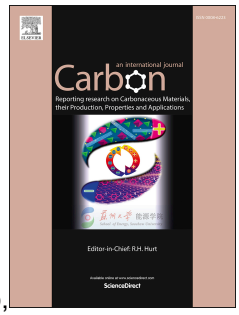

Aligning graphene in bulk copper: Nacre-inspired nanolaminated architecture coupled with in-situ processing for enhanced mechanical properties and high electrical conductivity

Mu Cao, Ding-Bang Xiong, Zhanqiu Tan, Gang Ji, Behnam Amin-Ahmadi, Qiang Guo, Genlian Fan, Cuiping Guo, Zhiqiang Li, Di Zhang

PII: S0008-6223(17)30219-1

DOI: 10.1016/j.carbon.2017.02.089

Reference: CARBON 11793

To appear in: *Carbon*

Received Date: 29 December 2016

Revised Date: 22 February 2017

Accepted Date: 25 February 2017

Please cite this article as: M. Cao, D.-B. Xiong, Z. Tan, G. Ji, B. Amin-Ahmadi, Q. Guo, G. Fan, C. Guo, Z. Li, D. Zhang, Aligning graphene in bulk copper: Nacre-inspired nanolaminated architecture coupled with in-situ processing for enhanced mechanical properties and high electrical conductivity, *Carbon* (2017), doi: 10.1016/j.carbon.2017.02.089.

This is a PDF file of an unedited manuscript that has been accepted for publication. As a service to our customers we are providing this early version of the manuscript. The manuscript will undergo copyediting, typesetting, and review of the resulting proof before it is published in its final form. Please note that during the production process errors may be discovered which could affect the content, and all legal disclaimers that apply to the journal pertain.

Graphical Abstract

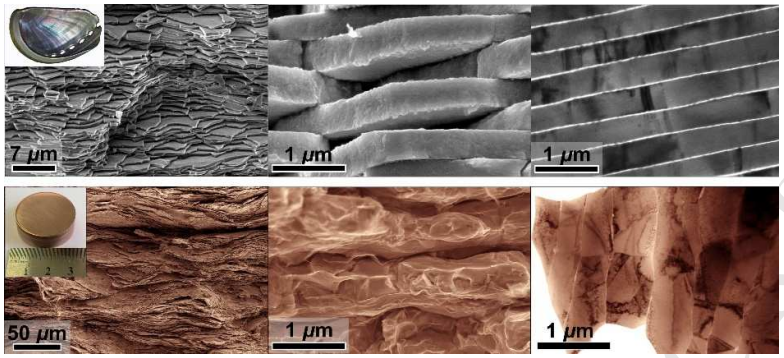

ACCEPTED MANUSCRIPT

ACCEPTED MANUSCRIPT

Aligning graphene in bulk copper: nacre-inspired nanolaminated architecture coupled with in-situ processing for enhanced mechanical properties and high electrical conductivity

Mu Cao [a], Ding-Bang Xiong [a,*], Zhanqiu Tan [a], Gang Ji [b], Behnam Amin-Ahmadi [c], Qiang Guo [a], Genlian Fan [a], Cuiping Guo [a], Zhiqiang Li [a], and Di Zhang [a,**]

[a] *State Key Laboratory of Metal Matrix Composites, Shanghai Jiao Tong University, Shanghai 200240, China*

[b] *Unité Matériaux et Transformations (UMET) CNRS UMR 8207, Université Lille1, 59655 Villeneuve d'Ascq, France*

[c] *Electron Microscopy for Materials Science (EMAT), University of Antwerp, Groenenborgerlaan 171, 2020- Antwerp, Belgium*

* Corresponding author. *E-mail address*: xiongdingbang@sjtu.edu.cn (Ding-Bang Xiong)

** Corresponding author. *E-mail address*: zhangdi@sjtu.edu.cn (Di Zhang)

ACCEPTED MANUSCRIPT

Abstract:

Methods used to strengthen metals generally also cause a pronounced decrease in ductility and electrical conductivity. In this work a bioinspired strategy is applied to surmount the dilemma. By assembling copper submicron flakes cladded with in-situ grown graphene, graphene/copper matrix composites with a nanolaminated architecture inspired by a natural nacre have been prepared. Owing to a combined effect from the bioinspired nanolaminated architecture and improved interfacial bonding, a synergy has been achieved between mechanical strength and ductility as well as electrical conductivity in the graphene/copper matrix composites. With a low volume fraction of only 2.5% of graphene, the composite shows a yield strength and elastic modulus ~177% and ~25% higher than that of unreinforced copper matrix, respectively, while retains ductility and electrical conductivity comparable to that of pure copper. The bioinspired nanolaminated architecture enhances the efficiencies of two-dimensional (2D) graphene in mechanical strengthening and electrical conducting by aligning graphene to maximize performance for required loading and carrier transporting conditions, and toughens the composites by crack deflection. Meanwhile, in-situ growth of graphene is beneficial for improving interfacial bonding and structural quality of graphene. The strategy sheds light on the development of composites with good combined structural and functional properties.

ACCEPTED MANUSCRIPT

1. Introduction

Analogous to that transforming crystal structure at atomic and molecular scale can lead to change in the properties of a compound, recently tailoring properties by architecture design that changes the spatial distribution of reinforcement in matrix at micro-/nano-scale without changing constituents has attracted intensive attention in the field of composites [1]. Natural biological materials are usually made up of only simple constituents, but show remarkable range of mechanical and functional properties, which can be attributed to multiscale transformation on their architectures [2-6]. Understanding the role that multilevel architectures play in controlling properties of natural materials may serve as inspirations for architecture design in composites.

Usually, conventional metal matrix composites (MMCs) containing homogeneously distributed reinforcement exhibit higher strength but compromise ductility and toughness compared to the pure matrix. In nature, the most typical example that surmounts the conflict between strength and toughness by architecture design is probably the nacreous part of seashells [7]. Nacre is made up of about 95 vol % brittle mineral aragonite (a polymorph of calcium carbonate) and only a few percent of soft organic material, however, it exhibits phenomenal fracture strength and toughness properties thanks to a perfectly ordered “brick-and-mortar” architecture [8]. For example, its work of fracture is three orders of magnitude greater than that of a single crystal of its constituent mineral aragonite [9]. Therefore, mimicking the unique “brick-and-mortar” architecture in nacre might be a promising strategy for producing MMCs with optimum combination of strength and ductility and toughness. Such bioinspired architecture could be built in MMCs by using high strength reinforcement with high aspect ratio as “brick” combined with ductile metal “mortar”. While “brick” of reinforcement is by no means easy to obtain, some emerging two-dimensional (2D) nanomaterials show great promise as ideal

candidates, such as graphene (Gr) [10,11], hexagonal boron nitride (*h*-BN) [12-14] and MXenes (derivatives of layered ternary carbides and nitrides known as MAX phases) [15,16]. They not only have outstanding intrinsic properties, but also are geometrically compatible with lamella in the "brick-and-mortar" structure. Meanwhile, these 2D nanomaterials exhibit high in-plane rigidity while large out-of-plane flexibility, and thus their strengthening efficiencies in composites are strongly affected by the way the individual sheets are arranged. Therefore, in the "brick-and-mortar" structure, 2D nanomaterials are parallel arranged and their strengthening capability could be fully exerted when a load is applied along the direction of their maximum performance [17].

Among the aforementioned 2D nanomaterials, graphene is the most investigated emerging nano-reinforcement for composites. Up to now, most of the studies on Gr/metal composite emphasize the homogeneous dispersion of graphene and the suppression of its restacking, but the orientation of graphene is random and out of control, such as in the Gr/metal composites fabricated through ball-milling [18-22], molecular-level mixing [23,24], slurry blending [25,26] and electrodeposition [27]. The major difficulties for dispersing graphene in a metal matrix lie in graphene restacking, structural damage as well as poor interfacial bonding. Because of its 2D atomic layer structure, graphene exhibits high surface energy, high aspect ratio and strong Van der Waals interaction, and is prone to agglomerate during its mixing with metal [22,28]. Therefore, graphene is usually dispersed in metal matrix by using a ball-milling method. However, high energy during ball-milling will lead to structural damage of graphene [29] and some adverse reactions at interface [30]. Moreover, wettability of graphene with metal has to be improved to enhance interfacial bonding strength [31]. Beyond above difficulties, for fabricating Gr/metal composites with the "brick-and-mortar" structure, additional bigger challenge is

alignment of graphene in metal matrix, because graphene is flexible and has large aspect ratio.

Recently, efforts have been made to fabricate metal matrix composites reinforced with aligned graphene (or reduced graphene oxide, rGO), demonstrating the advantage from the resulting nanolaminated structure in strengthening and toughening the composites, but these fabrication processes are relatively complicated and difficult to be scaled-up [32-34]. To fabricate bulk Gr/metal nanolaminated composites for large-scale applications, flake powder metallurgy has been established in our group in the past few years [35-39]. It is a bottom-up assembly process of composite flaky powders, i.e. nanoflake metal powders covered with rGO were used as building blocks to be orderly assembled together forming composites. This strategy has made a great success in strengthening and toughening lightweight Al matrix composites. Nevertheless, some major issues are not fully understood and addressed yet. Firstly, it remains a challenge to evaluate the rGO's individual contribution in strengthening and toughening composite, because Al is chemically active and Al_2O_3 passivation layer inevitably forms during preparing Al nanoflakes via a ball-milling process [35,40,36]. Secondly, although catalytically grown graphene has better intrinsic mechanical and functional properties than graphene oxide (GO, usually produced by chemical methods) [41-43], it is GO that is used more often in reinforcing metal matrix because of its lower fabrication cost and easy handling. Therefore, a strategy is desired to incorporate catalytically grown graphene in such bioinspired nanolaminated composites for further improving overall performance. Thirdly, in contrast to intensive investigations on mechanical properties, functional properties in such bioinspired composites remain largely unexplored, while a synergy between them is required for more and more emerging applications.

Motivated by the aforementioned major issues, nacre-inspired Cu matrix nanolaminated composites reinforced with in-situ catalytically grown graphene were prepared in this study. Cu matrix composite has been intensively investigated for both structural and functional purposes [44,45]. Unlike chemically active Al, copper oxide impurities are easy to be reduced. Moreover, Cu is a typical catalyst for growing graphene, and Cu in various forms can be used for this purpose, such as foil [46], nanowire [47], particle [48-51] and porous Cu [52,53]. Here, Cu submicron flakes cladded with in-situ catalytically grown graphene were used as the building block for fabricating bulk Gr/Cu composite with the bioinspired nanolaminated structure via a bottom-up assembly process. Tensile test on the as-obtained composites reveals that graphene in the nanolaminated composites shows remarkably higher strengthening and stiffening efficiencies than those of other reinforcements, while the composites retains a ductility and electrical conductivity comparable to that of pure Cu. The superior overall performance is interpreted in terms of architecture effect, interfacial bonding and interaction between graphene and Cu matrix. This work highlights the importance of architecture design in developing composites with good combined structural and multifunctional properties.

2. Experimental methods

2.1. Fabrication of Cu flaky powders

100 g of commercially available spherical Cu powders (99.99% purity, with an averaged particle size of 40 μm) were ball milled in a stainless steel mixing jar at a speed of 423 rpm for 5 h in pure ethanol, with a mass ratio between the Cu powder and the stainless steel milling ball of about 1:20.

2.2. In-situ fabrication of graphene/Cu flaky composite powders

30g as-prepared Cu flaky powders were mixed with 250 ml 0.05~0.5 wt% Poly(methyl methacrylate) (PMMA) (M.W. 35000,) anisole solution. The slurry was stirred for 12 h, and then centrifuged at 4000 rpm for 10 min. The obtained PMMA/Cu flaky powders were dried in a vacuum oven at 85 ºC for 2 h to remove the solvent. The PMMA coated Cu flaky powders were put in an aluminum crucible and were heated in a tube furnace. Temperature was rapidly elevated to 900ºC under H_2 (100 sccm) and Ar (400 sccm) flow at atmospheric pressure and then kept at this temperature for one hour. The Gr/Cu composite powders were obtained by fast-cooling to room temperature under the H_2/Ar atmosphere.

2.3. Characterization of Gr/Cu flaky composite powders

Graphene was detached from the composite powder by etching the Cu substrate in a ferric chloride aqueous solution, then filtered and washed by water and ethanol, and finally dried in 60 ºC. Raman spectroscopy (Bruker Optics Senterra R200-L) was performed by using Ar^+ laser with a wavelength of 532 nm as excitation source to characterize structural integrity of graphene in composite powder. X-ray photoelectron spectroscopy (XPS, Kratos AXIS UltraDLD) was used to characterize elemental composition and chemical bonding. The morphology and distribution of graphene on the surface of Cu flaky powder were characterized by scanning electron microscope (SEM, Hitachi S-4800).

2.4. Consolidation of Gr/Cu composite powders

The Gr/Cu flaky composite powders were assembled in a graphite die (Ø30 mm) and then compacted in hot-pressing furnace. The powders were sintered in Ar atmosphere at 900 ºC and 50 MPa for 20 min under a heating rate of 15 ºC/min. The hot-pressed Gr/Cu composites were then hot-rolled with a reduction of 70% at 850 ºC for mechanical and electrical characterizations.

2.5. Characterization of nacre-inspired Gr/Cu nanolaminated composite

Microstructure characterization of the Gr/Cu nanolaminated composite was performed using SEM and HR-TEM, (JEOL JEM-2100F). The tensile testing was carried out on universal testing machine (Zwick/Roell Z100). Electrical conductivity was tested by four point probe instrument (Ecopia EPS-300), and all the samples were wire-cut into a dimension of 10 mm × 5 mm × 0.2 mm and polished by 0.5-μm Al_2O_3 sandpaper to avoid the influence of rough surface on conductivity measurement. Roughness of fractured surface was characterized by 3D optical surface profile (ZeGage 3D Optical Surface Profiler).

2.6. Synthesis of Cu/Gr/Cu model materials and its interfacial tensile test

The model material was made of two pieces of copper foil and graphene in the middle. Graphene was introduced on the surface of a 45-μm thick Cu foil (20 mm × 10 mm) by using a chemical vapor deposition (CVD) method, and the coverage was over 95%. The sandwiched Cu-foil/Gr/Cu-foil was obtained by sintering (700ºC and 50 MPa) the CVD Gr/Cu foil with one piece of annealed Cu foil (suffered the same temperature condition in the CVD process). A controlled sample of Cu-foil/GO/Cu-foil was prepared by sintering a GO covered Cu foil with another annealed Cu foil. GO aqueous solution was spread on the surface of annealed Cu foil and then dried. 0.05 wt% GO aqueous solution was used and adsorption time was optimized to control the coverage of one-layer graphene oxide over 95%. Interfacial tensile tests on the model composites were carried out on universal testing machine at a constant rate of 1.0 mm/min at room temperature until the two pieces of Cu foil was completely separated.

3. Results and discussion

3.1. Synthesis and Microstructural Characterization

The fabrication process used to make nacre-inspired Gr/Cu composites is illustrated in **Fig. 1**.

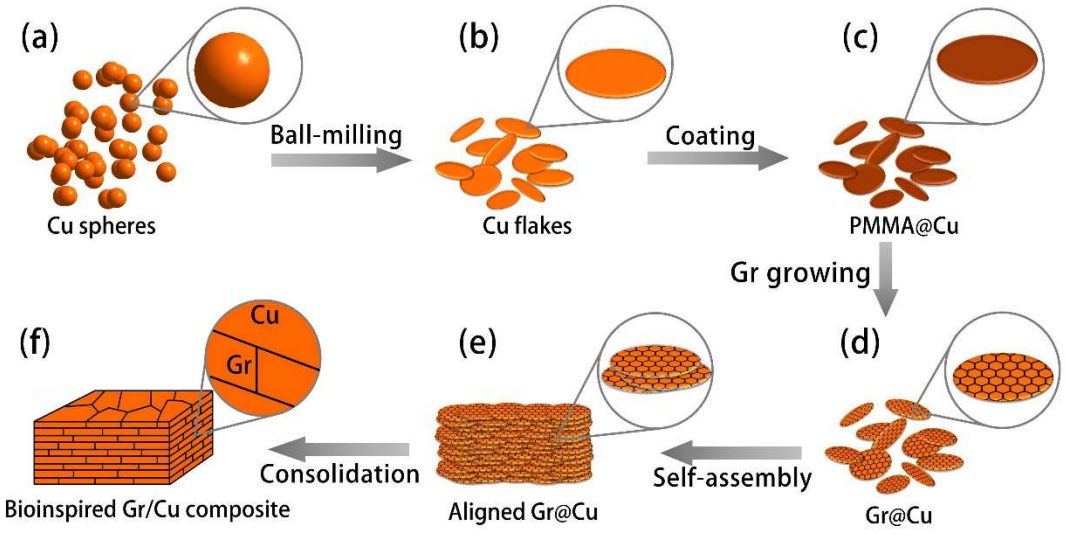

Fig. 1. Schematic illustration of fabrication of Gr/Cu composite with nacre-inspired structure. Spherical Cu powder (a) were first transformed into Cu flake (b) by a ball-milling process. (c) The as-obtained Cu flakes were soaked in an anisole solution of PMMA (typically less than 1wt %) and then dried in vacuum, forming a uniform PMMA film on the surface. (d) The coated PMMA was used as carbon source for in-situ growing graphene at elevated temperature. (e) The Gr/Cu composite powders were self-assembled into green compact by gravity because of its large aspect ratio. (f) A nacre-inspired composite was finally obtained by a hot-pressing and hot-rolling process.

First, starting from spherical Cu powder (**Fig. 1**a), Cu flakes (**Fig. 1**b) were obtained by using a ball-milling method. The thickness of Cu flakes could be controlled by adjusting ball-milling time and rotating speed. PMMA was coated on the surface of Cu flakes (**Fig. 1**c) and used as the carbon source for graphene growth. Cu is a typical catalyst for growing graphene, and it acts as

both catalyst and matrix in this study. By heating the PMMA coated Cu flakes at elevated temperature in a tube furnace under H_2/Ar flow (20 vol % H_2), graphene was grown on the surface to form Gr/Cu composite flakes (**Fig. 1**d). The layer number of grown graphene could be controlled by adjusting the concentration of PMMA solution in the coating process, and few layer graphene could be obtained with a concentration less than 1 wt%. Under uniaxial compaction at room temperature, the as-obtained Gr/Cu composite flakes self-assembled into green compact with an orderly laminated structure owing to their large aspect ratio (**Fig. 1**e). A vacuum filtration can promote the formation of laminated structure. The aspect ratio and thickness of the flakes have a decisive role on the final architecture, and ball-milling parameters have to be optimized for a nanolaminated composite. Finally, fully densified Gr/Cu bulk composites with a bioinspired nanolaminated structure were produced via vacuum hot pressing and hot rolling (**Fig. 1**f). Details of the fabrication process and microstructure evolution can be found in Experimental section and Supporting Information (**Fig. S1**).

The as-obtained Gr/Cu composite powders were characterized by scanning electron microscopy (SEM), Raman spectroscopy and X-ray photoelectron spectroscopy (XPS) (see **Fig. S2-4** in the Supporting Information). As observed by SEM, grain boundaries in the Cu flakes are clearly seen beneath the as-grown graphene, and even twin boundaries can be distinguished in graphene/Cu flakes prepared from low PMMA concentrations, indicating few-layer graphene with high light transmission is obtained [54]. To explore the quality of in-situ grown graphene, graphene was detached from the composite powder by etching Cu in a ferric chloride aqueous solution and characterized by Raman spectroscopy. The relative intensity between the D and G peaks (I_D/I_G) reflects the quality of graphene, and was measured to be 0.24 and 0.62 for two representative flakes. The values are significantly smaller than that of most graphene oxide,

indicating lower defect concentration in catalytically grown graphene. Furthermore, XPS scans confirmed the sp^2-hybridized carbon orbitals of graphene [55]. The bonding characteristics were analyzed based on high resolution XPS, indicating no chemical bonding between graphene and Cu in the as-obtained

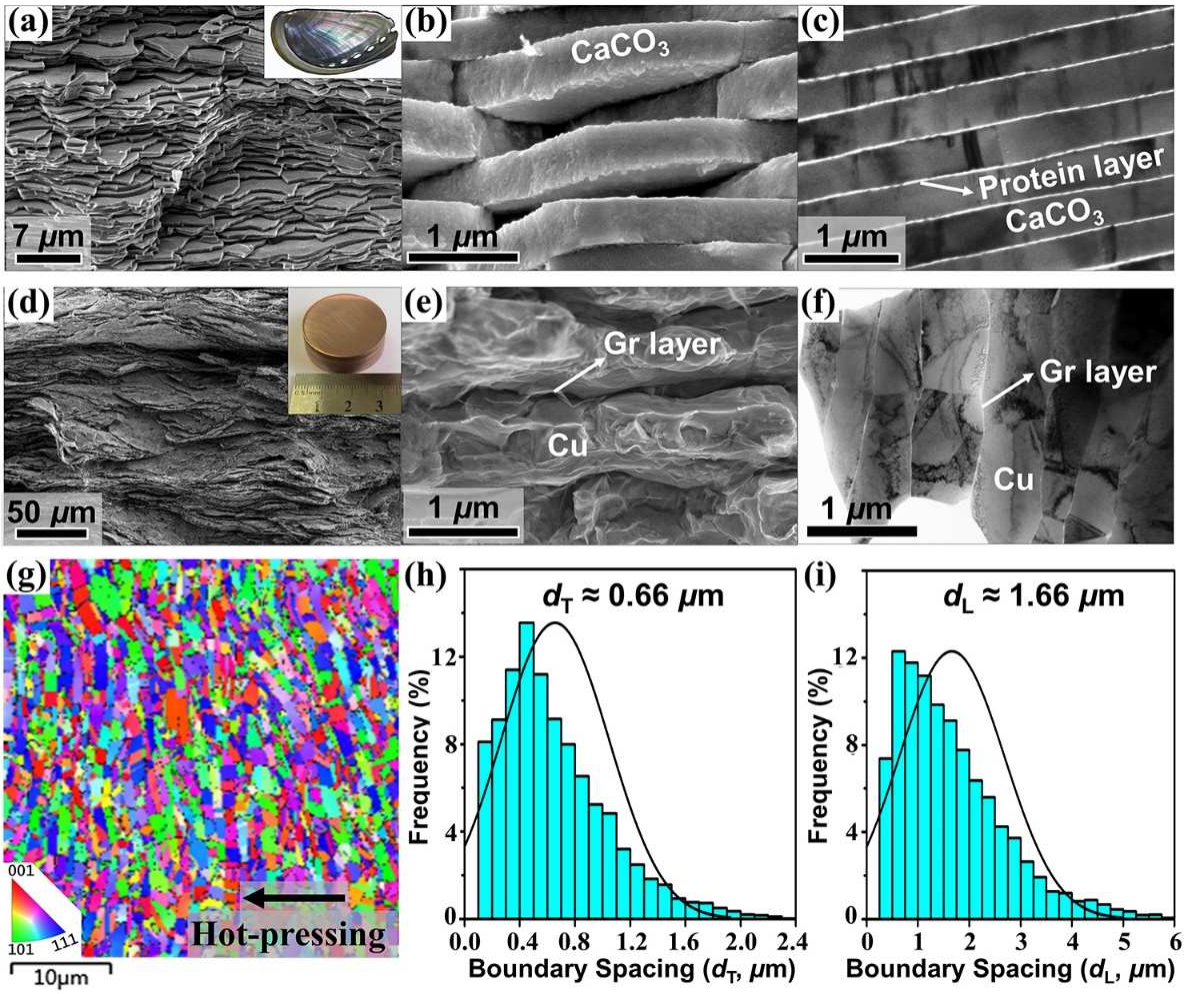

Fig. 2. Structure of nacre-inspired Gr/Cu composite compared to natural nacre. Panels (a–c) correspond to nacre; panels (d–f) to nacre-inspired Gr/Cu composite. The as-obtained Gr/Cu composites show a similar "brick-and-mortar" structure as that in natural nacre. (a,d) SEM micrographs showing the long-range order of flakes, and (b,e) local stacking of flakes. The insets in (a,d) are nacre and densified Gr/Cu composite, respectively. (c,f) TEM micrographs showing

local stacking of flakes. (g) An EBSD image of the cross-section of the nacre-inspired Gr/Cu composite, revealing a laminated structure, from which boundary spacings of the elongated Cu grains were estimated. (h,i) Distribution of the boundary spacing parallel (d_T) and perpendicular (d_L) to the hot-pressing direction. At least 150 boundaries were measured and statistically averaged.

Gr/Cu composite powders. Weak interaction between graphene and Cu in an as grown CVD Gr/Cu foil is confirmed by a low adhesion energy value of ~0.72 J m^{-2} obtained from a double cantilever beam (DCB) test on the interface [56]. The measured value is close to other such values calculated through quantum simulations according to a van der Waals interaction [57,58].

Fig. 2 highlights strong similarities at several length scales between natural nacre (**Fig. 2**a-c) and the Gr/Cu composites after a hot-processing process (**Fig. 2**d-f), validating the possibility to fabricate bulk, centimeter-sized or even larger samples with only a few simple processing steps. In natural nacre, ~500 nm thick platelets of mineral aragonite are compared to “bricks”, bonded by ~10 nm thick protein mortar in-between, resulting in a regular “brick-and-mortar” structure. The final microstructure of nacre-inspired Gr/Cu composite is characterized by a dense stacking of lamellae presenting long-range order, in which 2D graphene and Cu flake are alternately stacked. Each Cu matrix lamella contains predominantly a single grain through its thickness. As revealed by the electron backscatter diffraction (EBSD) analysis, no obvious crystallographic texture exists in hot-pressed composites (**Fig. 2**g). The distribution of boundary spacing scaled by the interception length along lines perpendicular (d_T) and parallel (d_L) to the hot-pressing direction is shown in **Fig. 2**h and **Fig. 2**i, respectively. The average sizes of the elongated grains are $d_T \approx 0.66$ and $d_L \approx 1.66$ μm. Without the confinement by graphene, the grains in the

unreinforced Cu matrix recrystallized and were found to be equiaxialed crystals with an average size of ~2.02 μm (see **Fig. S5** in the Supporting Information).

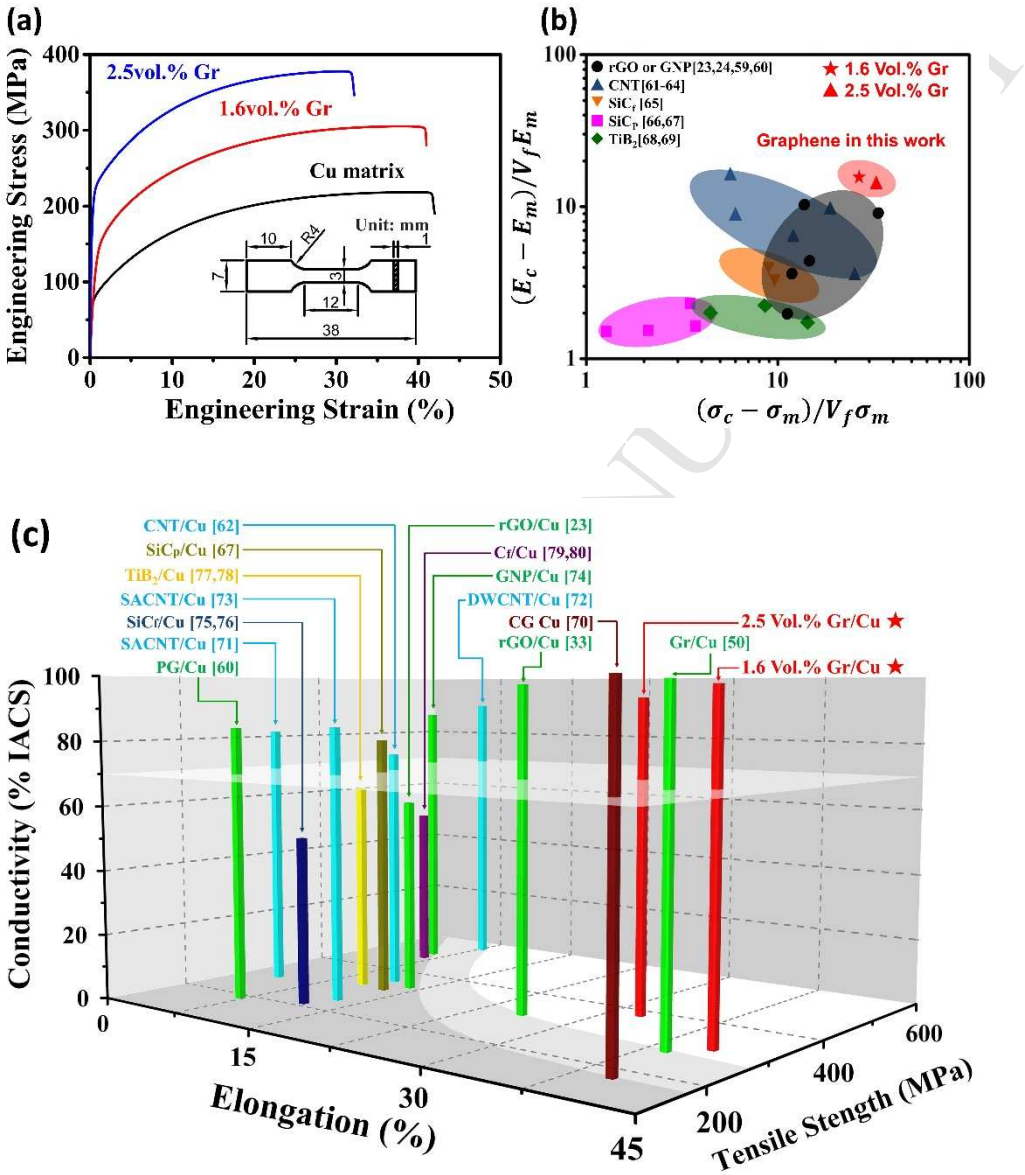

Fig. 3. Tensile properties and electrical conductivity of Gr/Cu composites. (a) Engineering stress-strain curves for Gr/Cu composites and the unreinforced Cu matrix. (b) Comparison of the strengthening and stiffening efficiencies of graphene in Gr/Cu composites with various reinforcements in other reported Cu matrix composites. (c) Comparison of overall properties

including tensile strength, elongation and electrical conductivity of the Gr/Cu composites with other reported Cu matrix composites. The curved shadows at the bottom indicate the conflict between strength and elongation.

Table 1. Tensile properties and electrical conductivity of the Gr/Cu nanolaminated composites and the unreinforced Cu matrix.

sample	yield strength (MPa)	tensile strength (MPa)	Young's modulus (GPa)	total elongation (%)	electrical conductivity (%IACS)[a]
Cu	72	218	108	43.5	97.8
1.6 vol %-Gr/Cu	122	305	127	41.0	97.1
2.5 vol %-Gr/Cu	200	378	135	32.3	93.8

[a]IACS is an acronym for international annealed copper standard, 58×10^6 S m^{-1} at 20 ^oC.

3.2. Mechanical and Electrical Properties

Tensile tests were performed to evaluate the strength, stiffness, and elongation of the rolled Gr/Cu composites. **Fig. 3**a shows representative engineering stress-strain curves of the nacre-inspired 1.6 and 2.5 vol % Gr/Cu nanolaminated composites (the volume fractions of graphene were estimated by measuring average thickness of graphene layer and Cu matrix layer in transmission electron microscope (TEM)), together with that of unreinforced Cu matrix fabricated using identical processing conditions but without graphene growth. Key mechanical data obtained from the tensile tests are summarized and tabulated in **Table 1**. 1.6 vol % Gr/Cu composite was shown to have a tensile strength of 305 ± 10 MPa and a Young's modulus of 127 ± 3 GPa, ~40% and ~18% higher than those of the Cu matrix, respectively. Tensile strength and

Young's modulus of the composite further increase to 378 ± 8 MPa and a Young's modulus of 135 ± 4 GPa (~73% and ~25% enhancement over the Cu matrix) when the graphene concentration increases to 2.5 vol %. These results clearly indicate that graphene is a highly effective reinforcement in the nacre-inspired nanolaminated composites. The high strengthening capability can be better presented by comparing its strengthening and stiffening efficiencies with those of Cu matrix composites reinforced by other reinforcements. The strengthening (or stiffening) efficiency of a reinforcement in a composite is defined as the strength (or modulus) increment per unit volume fraction of the reinforcement, *i.e.*, $(\sigma_c - \sigma_m)/V_f\sigma_m$ and $(E_c - E_m)/V_fE_m$, where σ_c and σ_m are the tensile strengths of the composite and the matrix, respectively, E_c and E_m are the Young's modulus of the composite and the matrix, respectively, and V_f is the volume fraction of the reinforcement. As shown in **Fig. 3**b, the strengthening and stiffening efficiencies of graphene in the nacre-inspired nanolaminated composites are considerably higher than those of conventional particle and fiber reinforcements, and also superior to those of carbon nanotube (CNT) as well as graphene (or its derivatives) in other Cu matrix composites reported so far [59-69].

The simultaneous attainment of both high strength, high ductility as well as high conductivity in metals is a vital requirement for many modern applications; unfortunately, methods used to strengthen metals generally also cause a pronounced decrease in ductility and electrical conductivity. In this work, the tensile tests show that the uniform elongation of 41 ± 1.5% for the 1.6 vol% Gr/Cu and 32.3 ± 1.6% for 2.5 vol% Gr/Cu nacre-inspired nanolaminated composites are moderately lower than that of pure Cu matrix (43.5 ± 0.7%). At the same time, the electrical conductivity of the composites is identical to that of the Cu matrix. As shown in **Fig. 3**c, a good balance between strength, ductility and conductivity has been achieved in the in-situ grown

Gr/Cu nacre-inspired nanolaminated composites [70-80].

3.3. Interface Structure and Bonding

Fig. 4a is a representative TEM image for the interface between graphene and the copper matrix, showing that the interfaces are free of impurities, voids, or gaps. The few-layer graphene (11 layers) shows a distinct lattice fringe with a 0.34 nm spacing of (0002) plane, confirming

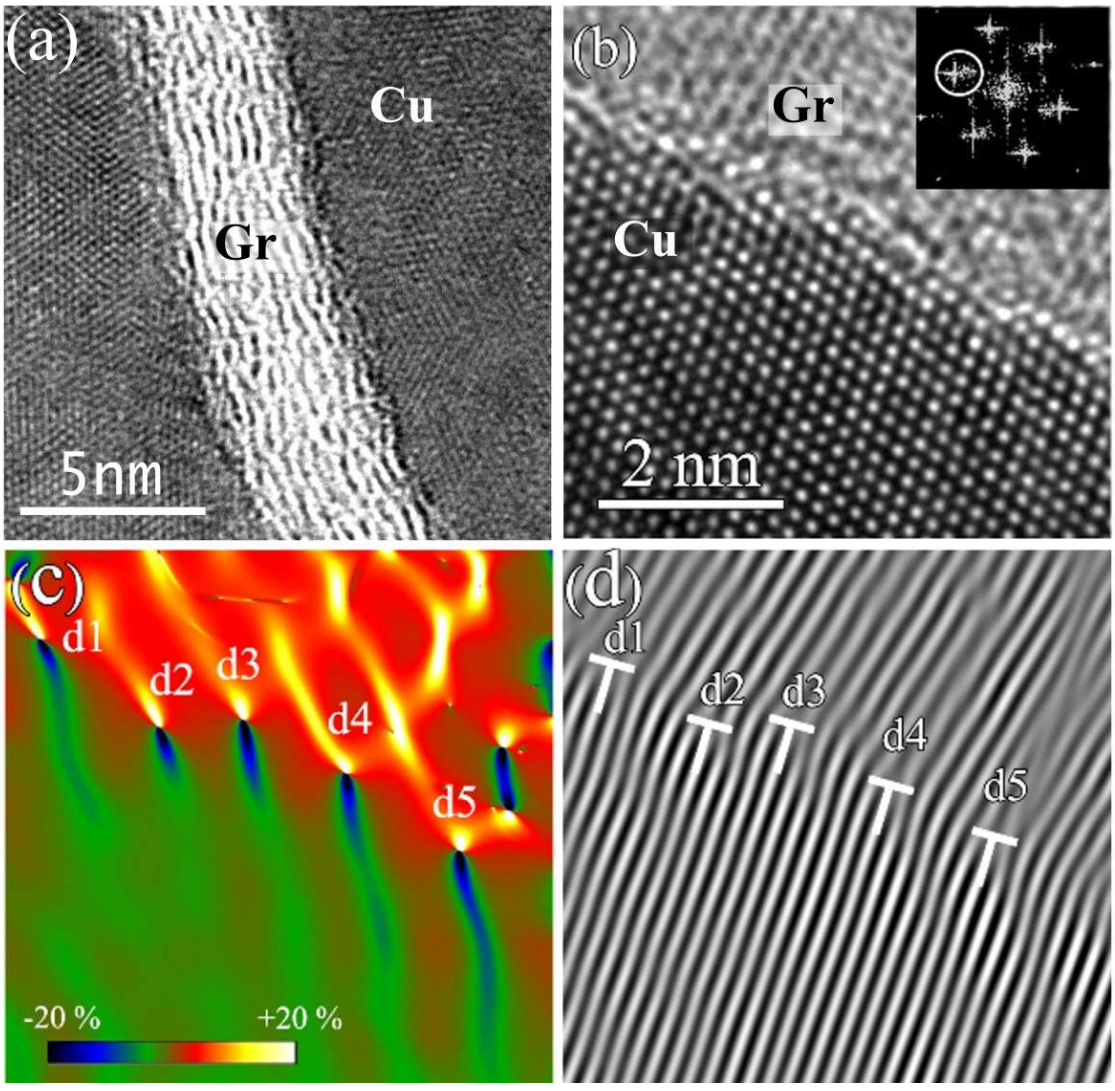

Fig. 4. Analyses on Gr/Cu interfaces. (a) TEM micrograph image showing the Gr/Cu interface. (b) High resolution TEM image of Gr/Cu interface along the [110] direction of Cu matrix. The

corresponding FFT is shown in the upper right inset. (c) GPA map (local ***g***-map) of the (b) showing the position of the misfit dislocations at the interface as hot spots. (d) Inverse FFT of one family of planes to show the position of dislocations indicated as extra half planes (pointed out by "T" symbols). Both local ***g***-map (c) and inverse FFT (d) were obtained using the ***g*** = {111} indicated by circle in the FFT inset of (b).

they are highly graphitized and of high quality. The thickness of graphene could be controlled by adjusting the carbon source concentration of PMMA solution, but obtaining graphene with less than five layers is still of challenge by using the solid carbon source (see **Fig. S6** in the Supporting Information). According to full atomistic nanoindentation simulations, Chang *et al* [81] reported that the hardness of the Ni/Gr/Ni sandwiched nanocomposites decreases with increasing the numbers of graphene layers (N). The weak Van der Waals interaction between graphene sheets is responsible for the reduction. In our cases, however, increasing N of in-situ grown graphene increases mechanical strength. The possible reason for the opposite conclusions may be the discrepancy between the volume fractions of graphene in the two works. In Chang's Ni/Gr/Ni sandwiched nanocomposites, the volume fraction of graphene ranges from 4.3 to 21 vol % (the number of graphene layer varies from N = 1 to N = 5 while the thickness of metal layer was kept constant as 8 nm), which is one order of magnitude higher than our samples (such as 1.6 and 2.5 vol %). When volume fraction of graphene is as low as that in this work, the strength increment contributed by increasing volume fraction can compensate the loss caused by the weak Van der Waals interaction between graphene nanosheets. However, for a fixed volume fraction of graphene (both high and low cases), Chang's conclusion suggests that graphene with fewer layers is beneficial for enhancing mechanical strength, because it means refinement of metal matrix layer (namely grain size) and reduction of adverse effect of weak Van der Waals

forces. Therefore, preparing a composite with thinner metal matrix layer thickness (λ) and less graphene layer number (N) is suggested [32].

As revealed by geometric phase analysis (GPA) map and inverse fast Fourier transform (FFT) image, misfit dislocations along the Gr/Cu interface could be easily visible. GPA is an image processing technique which is sensitive to small displacements of the lattice fringes in high-resolution TEM (HR-TEM) images and dislocations are shown as hot-spots [82]. **Fig. 4**b shows a typical HR-TEM image of the Gr/Cu interface along the [110] zone axis of Cu matrix in the as-obtained nacre-inspired composites. The corresponding FFT was also shown in upper right inset of **Fig. 4**b. **Fig. 4**c shows the corresponding GPA evaluation on **Fig. 4**b. The color map represents the strain component according to the ε_{xy} [111] direction. Most part of the graphene shows uniform strain and no strain difference, which is chosen as the reference frame. The matrix has a color between red and green, corresponding to about –16% lattice strain when compared with the reference, which is too large for a lattice accommodation via elastic strain. Indeed, as seen in the corresponding inverse FFT image (**Fig. 4**d) of one family of planes (shown by a circle in the FFT inset in **Fig. 4**b), periodic interface mismatch dislocations can be clearly recognized as extra half planes which are indicated by “T” symbols. Such lattice mismatch dislocations between the graphene and the Cu matrix occur every five or six {111} planes, namely 16~20% mismatch, corresponding to the ~16% lattice strain estimated from the color map (**Fig. 4**c). The misfit dislocation with high density at interface plays an important role in strengthening nacre-inspired Gr/Cu composites because of stronger interaction between dislocations during metal deformation.

Interface bonding is of great importance in composites because it affects the load-transfer and energy-exchange efficiency between reinforcement and matrix. As far as we know, graphene and

its derivatives have been used as reinforcements in metal matrix composites, but no direct experimental data has been reported to compare their relative interface bonding strength in composites. Conventional methods such as push-out and pull-out are effective for measuring the interface bonding strength of traditional ceramic and carbon micro-fiber reinforcement in composites, but they are of great challenge [83] or even impossible for flexible nano

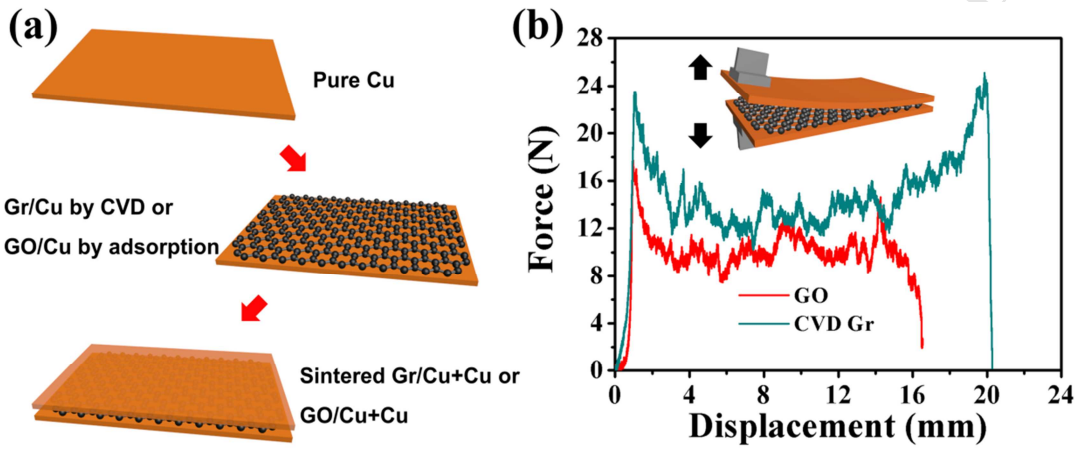

Fig. 5. (a) Schematic illustration of fabrication process of Cu-foil/Graphene/ Cu-foil and Cu-foil/Graphene oxide/Cu-foil specimens for interface tensile testing. (b) Comparison on interface bonding strength in the composites reinforced with CVD graphene and adsorped graphene oxide.

reinforcements such as carbon nanotube and graphene. Recently, Hwang *et al* reported the direct measurement of adhesion energy between CVD graphene and Cu in a Cu-foil/Gr/Cu-foil sandwiched model composite by using a DCB fracture test [23].

Here, to compare the relative value of interface bonding strength between catalytically grown graphene and graphene oxide, a simplified interface tensile testing based on DCB was carried out on two model composites of Cu-foil/CVD Gr/Cu-foil and Cu-foil/GO/Cu-foil. **Fig. 5**a shows the fabrication process for the two model composites. Monolayer of both CVD graphene and graphene oxide were used to ensure that the interface bonding strength between the graphene and

Cu, but not between graphene layers, was measured. The graphene coverage rate on Cu foil in two model composites was also controlled to be commensurate with each other and above 95% for comparable fraction of graphene/Cu interface. Although no precise value of adhesion energy as in the standard DCB fracture test was measured, relative interface bonding strength was compared in these two model composites as indicated by force-displacement curves obtained under the same testing conditions (**Fig. 5**b). The energy required to separate the bonded Cu foils can be roughly estimated based on the area under the force-displacement curves, and the result shows that the energy for the interface with CVD graphene is about 80% higher than that for the interface with graphene oxide. The difference on interface bonding strength can be also appreciated by comparing the fractured surfaces (see **Fig. S7** in the Supporting Information). The fractured interface with CVD graphene is very rough and shows many ravines, which means interface bonding is strong enough to cause failure of Cu matrix during detachment, while the fractured interface with graphene oxide is smoother than the former. The adhesion energy between graphene and Cu as grown from CVD can be enhanced after sintering at high temperature and high pressure, which was explained by the existence of native oxygen on Cu and the formation of strong oxygen mediated carbon-Cu covalent bonding [23]. Along this line of consideration, the bonding strength in the interface with graphene oxide would be stronger than that with CVD graphene because of higher oxygen content, but the conclusion is reverse in our measured data. A possible reason might be the difference between lateral sizes of CVD graphene and graphene oxide. The lateral size of CVD graphene is about 10~20 μm, an order of magnitude larger than that of the graphene oxide prepared by the Hummers' method. It need more energy to tear a continuous CVD graphene than fragmented graphene oxide. The difference on lateral size makes the comparison complicated, but it implies that larger lateral size of graphene can

compensate the loss of interface bonding strength owing to the absence of bridge oxygen as that in graphene oxide. Moreover, the catalytically grown graphene has better intrinsic mechanical and functional properties than graphene oxide.

3.4. Fracture Behavior

Fig. 6 shows fracture surface for the nacre-inspired Gr/Cu composites and pure Cu matrix. The pure Cu sample shows well-developed dimples over the entire fractured surface, indicating a typical ductile fracture with high plastic deformation. No laminated structure was found in the pure Cu sample because of grain growth during consolidation at high temperature. With introducing graphene and increasing its volume fraction, the nacre-inspired nanolaminated structure was formed. As we can see from the fracture surface morphology, there is no graphene pull-out on the fractured surface, which is different from other reported graphene oxide reinforced metals [33]. The different facture behavior could be understood by a simple shear lag model [84]. The failure behavior (either pull-out or fracture of reinforcement) is determined by its relative size compared to the ratio of tensile strength of reinforcement to the yield shear strength of matrix. In this work, the yield shear strength of Cu matrix should have no substantial difference with that in other reported composites, and the difference might originate from competition between the strength and size of graphene. Compared to the reduced graphene oxide used in most reported metal matrix composites, the graphene in this work has higher structural integrity and therefore higher tensile strength, which means a larger critical aspect ratio in the Gr/Cu composites. On the other hand, as estimated from the surface morphology analysis on the Gr/Cu flaky powder from SEM images, the lateral size of the graphene here is on the scale of several micrometers at least. This size is remarkably larger than that of the graphene oxide used in most reported composites, resulting in a predominant failure behavior of graphene fracture but

not pulling-out.

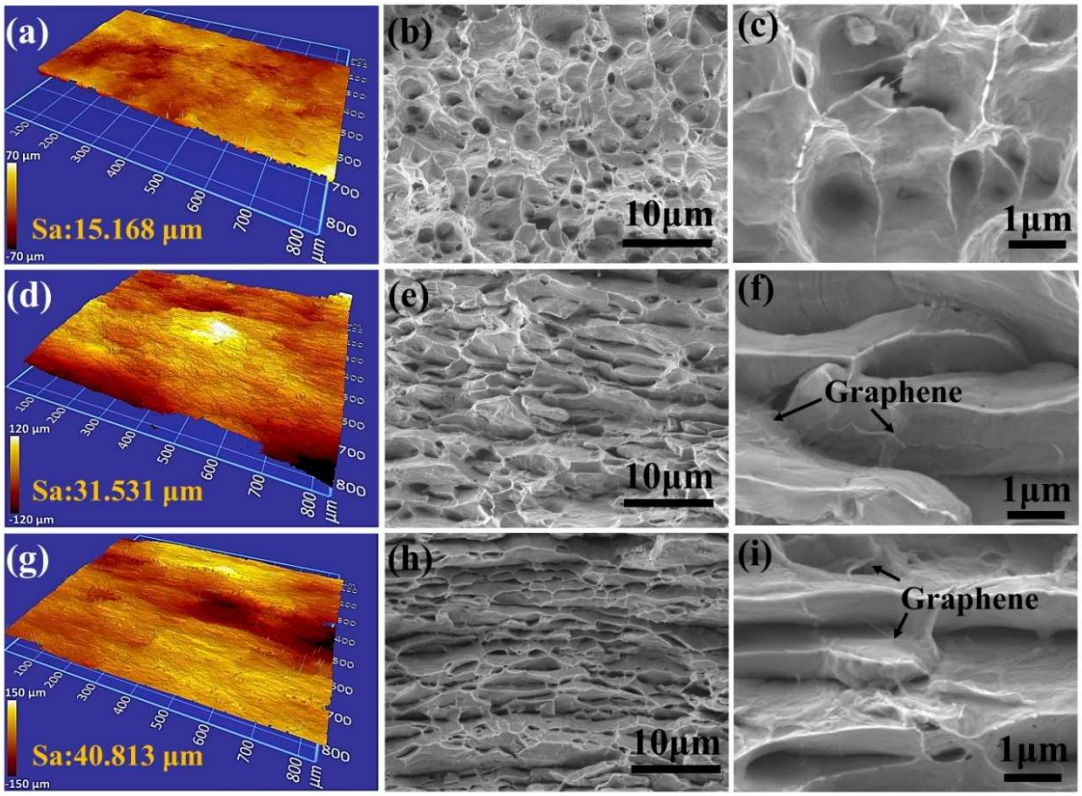

Fig. 6. Fractured surface analysis on (a-c) unreinforced copper matrix, (d-f) 1.6 vol % Gr/Cu, and (g-i) 2.5 vol % Gr/Cu by using 3D optical surface profiler (the left column) and SEM with low magnification (the middle column) and high magnification (the right column). The value of Sa in the left column is a 3D roughness parameter based on arithmetic mean height in the measured area.

3D optical surface profile was used to compare the fractured surface roughness in three samples. As indicated by the value of Sa (see **Fig. S8** in the Supporting Information), calculated from the arithmetic mean amplitude of fractured surface fluctuation, substantial discrepancy on surface roughness was measured between the three samples (**Fig. 6**a, d, g). As compared to unreinforced copper matrix, the nacre-inspired nanolaminated architecture caused an increase on

ACCEPTED

surface roughness by 108% and 161% in the 1.6 vol % Gr/Cu and 2.5 vol % Gr/Cu, respectively, indicating that the bioinspired architecture increased the total fracture surface area in the composites and therefore resulted in greater energy absorption as compared to an unreinforced matrix.

3.5. Discussions

The advantage of the nacre-inspired nanolaminated structure for balancing mechanical properties and electrical conductivity lies in both architecture effect and improved interface bonding (**Fig. 7**). The nacre-inspired nanolaminated architecture provides extrinsic toughening by crack deflection as indicated by increased fractured surface area. Meanwhile, with this

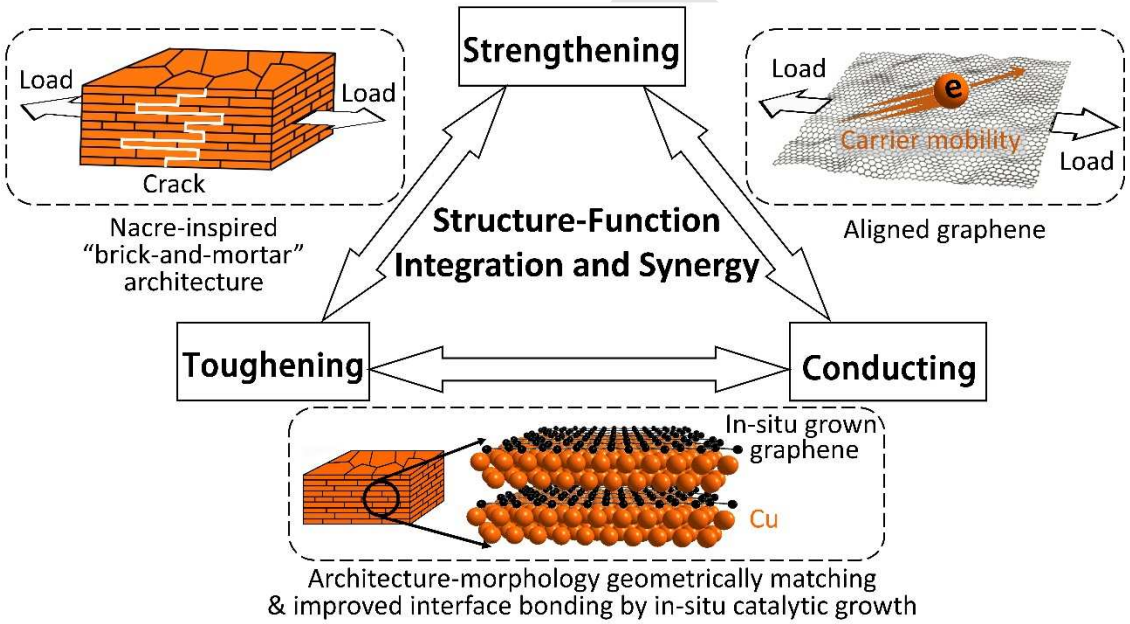

Fig. 7. Structure-function integration and synergy benefit from bioinspired nanolaminated architecture coupled with improved interface bonding in Cu matrix composite reinforced with in-situ grown graphene. Nanolaminated architecture not only toughen the composite by deflecting crack propagation, but also align graphene to maximize its performance for required loading and carrier transporting conditions. The in-situ catalytic growth process provides high structural

quality and enhanced interface bonding strength after sintering.

nanolaminated architecture, aligning graphene along the direction for required loading and carrier transporting conditions facilitates the load transfer between graphene and Cu matrix as well as enhancement on electrical conductivity. At the same time, the presence of high surface area graphene increases thermal stability of the nanolaminated structure and retains it during its hot-pressing and rolling at high temperature, while the grains coarsen in the pure Cu without graphene. The overall properties are expected to be further enhanced by optimizing the geometrical parameters, such as the layer number of grown graphene and the thickness of Cu matrix lamella. The former could be adjusted by using a gas carbon source, while the latter controlled by varying the conditions of ball-milling and deformation processing.

Another characteristic is the multipole role of Cu, acting as both the catalyst of growing graphene and metal matrix in the composites. Catalytically grown graphene is desired because higher structural quality as well as improved interface bonding. In general, the wettability of pure Cu on carbon is poor [85], making it difficult to disperse graphene in Cu and to form strong bonding with Cu matrix via casting or ball-milling processes, which could be resolved by in-situ growing graphene on Cu flakes. Moreover, this bioinspired strategy provides an idea for alignment and assembly of graphene in metal matrix. Also, this strategy could be extended to other metal catalysts that can be used for growing graphene, such as Fe, Co, Ni and their alloys as well as some noble metals, and scaled up for mass production because it is compatible with conventional powder metallurgy technology.

4. Conclusions

In this work, we have fabricated in-situ catalytically grown Gr/Cu composites with nacre-

inspired nanolaminated architecture. The resulting composites show a synergy between mechanical strength, elongation, elastic stiffness and electrical conductivity. The bioinspired nanolaminated architecture toughens the composite by crack deflection, strengthens the composites and retains electrical conductivity by alignment of 2D catalytically grown graphene to maximize its performance for required loading and carrier transporting conditions. Meanwhile, in-situ grown graphene improves interface bonding and structural quality. The strategy could be extended to other metal matrixes and multifunctional materials for thermal conductivity, tribological and electrical contact applications, shedding light on developing metal matrix composites with good combined structural and multifunctional properties.

Acknowledgments

The authors would like to acknowledge the Natural Science Foundation of China (Nos.51371115, 51671130, 51131004), the Ministry of Science & Technology of China (973 program, No.2012CB619600), Shanghai Science & Technology Committee (Nos.14JC1403300, 14DZ2261204, 15JC1402100, 14520710100).

Appendix A. Supplementary data

Supplementary data related to this article can be found at ……..

References

[1]. L. J. Huang, L. Geng, H. X. Peng, Microstructurally inhomogeneous composites: Is a homogeneous reinforcement distribution optimal?, Prog. Mater. Sci. 71 (2015) 93-168.

[2]. U. G. K. Wegst, H. Bai, E. Saiz, A. P. Tomsia, R. O. Ritchie, Bioinspired structural materials, Nat. Mater. 14 (1) (2015) 23-36.

[3]. M. A. Meyers, J. McKittrick, P. -Y. Chen, Structural biological materials: critical mechanics-materials connections, Science 339(6121) (2013) 773-779.

[4]. J. W. C. Dunlop, P. Fratzl, Multilevel architectures in natural materials, Scripta Mater. 68 (1) (2013) 8-12.

[5]. A. R. Studart, Towards High-Performance Bioinspired Composites, Adv. Mater. 24 (37) (2012) 5024-5044.

[6]. Q. F. Cheng, L. Jiang, Z. Y. Tang, Bioinspired layered materials with superior mechanical performance, Acc. Chem. Res. 47 (4) (2014) 1256-1266.

[7]. L. B. Mao, H. L. Gao, H. B. Yao, L. Liu, H. Cölfen, G. Liu, et al., Synthetic nacre by predesigned matrix-directed mineralization, Science 354 (6308) (2016) 107-110.

[8]. H. J. Gao, B. H. Ji, I. L. Jäger, E. Arzt, P. Fratzl, Materials become insensitive to flaws at nanoscale: lessons from nature, Proc. Natl. Acad. Sci. U.S.A. 100 (10) (2003) 5597-5600.

[9]. A. P. Jackson, J. F. V. Vincent, R. M. Turner, The mechanical design of nacre, Proc. R. Soc. London Ser. B 234 (1277) (1988) 415-440.

[10]. K. S. Novoselov, V. I. Fal'ko, L. Colombo, P. R. Gellert, M. G. Schwab, K. Kim, A roadmap for graphene, Nature 490 (7419) (2012) 192-200.

[11]. Q. F. Cheng, J. L. Duan, Q. Zhang, L. Jiang, Learning from nature: constructing integrated graphene-based artificial nacre, ACS Nano 9 (3) (2015) 2231-2234.

[12]. C. Y. Zhi, Y. Bando, C. C. Tang, H. Kuwahara, D. Golberg, Large-scale fabrication of boron nitride nanosheets and their utilization in polymeric composites with improved thermal and mechanical properties, Adv. Mater. 21 (28) (2009) 2889-2893.

[13]. D. Golberg, Y. Bando, Y. Huang, T. Terao, M. Mitome, C.C. Tang, et al., Boron nitride nanotubes and nanosheets, ACS Nano 4 (6) (2010) 2979-2993.

[14]. L. Boldrin, F. Scarpa, R. Chowdhury, S. Adhikari, Effective mechanical properties of hexagonal boron nitride nanosheets, Nanotechnology 22 (50) (2011) 505702.

[15]. B. Anasori, Y. Xie, M. Beidaghi, J. Lu, B. C. Hosler, L. Hultman, et al., Two-dimensional, ordered, double transition metals carbides (MXenes), ACS Nano 9 (10) (2015) 9507-9516.

[16]. M. Naguib, V. N. Mochalin, M. W. Barsoum, Y. Gogotsi, 25th anniversary article: MXenes: a new family of two-dimensional materials, Adv. Mater. 26 (7) (2014) 992-1005.

[17]. P. W. Liu, Z. Jin, G. Katsukis, L. W. Drahushuk, S. Shimizu, C. J. Shih, et al., Layered and scrolled nanocomposites with aligned semi-infinite graphene inclusions at the platelet limit, Science 353 (6297) (2016) 364-367.

[18]. S. E. Shin, D. H. Bae, Deformation behavior of aluminum alloy matrix composites reinforced with few-layer graphene, Compos. Part. A 78 (2015) 42-47.

[19]. W. J. Kim, T. J. Lee, S. H. Han, Multi-layer graphene/copper composites: Preparation using high-ratio differential speed rolling, microstructure and mechanical properties, Carbon 69 (2014) 55-65.

[20]. S. E. Shin, H. J. Choi, J. H. Shin, D. H. Bae, Strengthening behavior of few-layered graphene/aluminum composites, Carbon 82 (2015) 143-151.

[21]. S. J. Yan, S. L. Dai, X. Y. Zhang, C. Yang, Q. H. Hong, J. Z. Chen, et al. Investigating aluminum alloy reinforced by graphene nanoflakes, Mater. Sci. Eng. A 612 (2014) 440-444.

[22]. J. L. Li, Y. C. Xiong, X. D. Wang, S. J. Yan, C. Yang, W. W. He, et al., Microstructure and tensile properties of bulk nanostructured aluminum/graphene composites prepared via cryomilling, Mater. Sci. Eng. A 626 (2015) 400-405.

[23]. J. Hwang, T. Yoon, S. H. Jin, J. Lee, T. S. Kim, S. H. Hong, et al., Enhanced mechanical properties of graphene/copper nanocomposites using a molecular-level mixing process, Adv. Mater. 25 (46) (2013) 6724-6729.

ACCEPTED MANUSCRIPT

[24]. D. D. Zhang, Z. J. Zhan, Strengthening effect of graphene derivatives in copper matrix composites, J. Alloys and Comp. 654 (2016) 226-233.

[25]. J. H. Liu, U. Khan, J. Coleman, B. Fernandez, P. Rodriguez, S. Naher, et al., Graphene oxide and graphene nanosheet reinforced aluminium matrix composites: Powder synthesis and prepared composite characteristics, Mater. Des. 94 (2016) 87-94.

[26]. X. Gao, H. Y. Yue, E. J. Guo, H. Zhang, X. Y. Lin, L. H. Yao, et al., Preparation and tensile properties of homogeneously dispersed graphene reinforced aluminum matrix composites, Mater. Des. 94 (2016) 54-60.

[27]. C. L. P. Pavithra, B. V. Sarada, K. V. Rajulapati, T. N. Rao, G. Sundararajan, A new electrochemical approach for the synthesis of copper-graphene nanocomposite foils with high hardness, Sci. Rep. 4 (2014) 4049.

[28]. K. Chu, C. C. Jia, Enhanced strength in bulk graphene-copper composites, Phys. Status Solidi A 211 (2014) 184–190.

[29]. R. Pérez-Bustamante, D. Bolaños-Morales, J. Bonilla-Martínez, I. Estrada-Guel, R. Martínez-Sánchez, Microstructural and hardness behavior of graphene-nanoplatelets/aluminum composites synthesized by mechanical alloying, J. Alloys Comp. 615 (2014) S578-S582.

[30]. S. F. Bartolucci, J. Paras, M. A. Rafiee, J. Rafiee, S. Lee, D. Kapoor, N. Koratkar, Graphene-aluminum nanocomposites, Mater. Sci. Eng. A 528 (2011) 7933-7937.

[31]. Z. Y. Zhao, R. G. Guan, X. H. Guan, Z. X. Feng, H. Chen, Y. Chen, Microstructures and properties of graphene-Cu/Al composite prepared by a novel proves through clad forming and improving wettability with copper. Adv. Eng. Mater. 17 (2014) 663-668.

[32]. Y. Kim, J. Lee, M. S. Yeom, J. W. Shin, H. Kim, Y. Cui, et al., Strengthening effect of

single-atomic-layer graphene in metal–graphene nanolayered composites, Nat. Commun. 4 (2013) 2114.

[33]. D. -B. Xiong, M. Cao, Q. Guo, Z. Q. Tan, G. L. Fan, Z. Q. Li, et al., Graphene-and-copper artificial nacre fabricated by a preform impregnation process: bioinspired strategy for strengthening-toughening of metal matrix composite, ACS Nano 9 (7) (2015) 6934-6943.

[34]. D. -B. Xiong, M. Cao, Q. Guo, Z. Q. Tan, G. L. Fan, Z. Q. Li, et al., High content reduced graphene oxide reinforced copper with a bioinspired nano-laminated structure and large recoverable deformation ability, Sci. Rep. 6 (2016) 33801.

[35]. Z. Li, Q. Guo, Z. Q. Li, G. L. Fan, D. -B. Xiong, Y. S. Su, Enhanced mechanical properties of graphene (reduced graphene oxide)/aluminum composites with a bioinspired nanolaminated structure, Nano Lett. 15 (12) (2015) 8077-8083.

[36]. Z. Li, G. L. Fan, Z. Q. Tan, Z. Q. Li, Q. Guo, D. -B. Xiong, et al., A versatile method for uniform dispersion of nanocarbons in metal matrix based on electrostatic interactions, Nano-Micro Lett. 8 (1) (2016) 54-60.

[37]. Z. Li, G. L. Fan, Q. Guo, Z. Q. Li, Y. S. Su, D. Zhang, Synergistic strengthening effect of graphene-carbon nanotube hybrid structure in aluminum matrix composites, Carbon 95 (2015) 419-427.

[38]. Z. Li, G. L. Fan, Z. Q. Tan, Q. Guo, D. -B. Xiong, Y. S. Su, et al., Uniform dispersion of graphene oxide in aluminum powder by direct electrostatic adsorption for fabrication of graphene/aluminum composites, Nanotechnology 25 (32) (2014) 325601.

[39]. J. Y. Wang, Z. Q. Li, G. L. Fan, H. H. Pan, Z. X. Chen, D. Zhang, Reinforcement with graphene nanosheets in aluminum matrix composites, Scripta Mater. 66 (8) (2012) 594-597.

[40]. L. Jiang, Z. Q. Li, G. L. Fan, D. Zhang, A flake powder metallurgy approach to Al_2O_3/Al

biomimetic nanolaminated composites with enhanced ductility, Scripta Mater. 65 (5) (2011) 412-415.

[41]. C. Mattevi, G. Eda, S. Agnoli, S. Miller, K. A. Mkhoyan, O. Celik, et al., Evolution of electrical, chemical, and structural properties of transparent and conducting chemically derived graphene thin films, Adv. Funct. Mater. 19 (16) (2009) 2577-2583.

[42]. C. Navarro-Gómez, M. Burghard, K. Kern, Elastic properties of chemically derived single graphene sheets, Nano Lett. 8 (7) (2008) 2045-2049.

[43]. Z.Z. Sun, Z. Yan, J. Yao, E. Beitler, Y. Zhu, J.M. Tour, Growth of graphene from solid carbon sources, Nature 468 (2010) 549-552.

[44]. A. Mortensen, J. Llorca, Metal matrix composites, Annu. Rev. Mater. Res. 40 (2010) 243-270.

[45]. D. B. Miracle, Metal matrix composites–from science to technological significance, Compos. Sci. Technol. 65 (15) (2005) 2526-2540.

[46]. X. S. Li, W. W. Cai, J. An, S. Kim, J. Nah, D. X. Yang, et al., Large-area synthesis of high-quality and uniform graphene films on copper foils, Science 324 (5932) (2009) 1312-1314.

[47]. R. Mehta, S. Chugh, Z. H. Chen, Enhanced electrical and thermal conduction in graphene-encapsulated copper nanowires, Nano Lett. 15 (3) (2015) 2024-2030.

[48]. T. S. Koltsova, L. I. Nasibulina, I. V. Anoshkin, V. V. Mishin, E. I. Kauppinen, O. V. Tolochko, e al., New hybrid copper composite materials based on carbon nanostructures, J. Mater. Sci. Eng. B 2 (4) (2012) 240-246.

[49]. S. L. Wang, X. L. Huang, Y. H. He, H. Huang, Y. Q. Wu, L. Z. Hou, et al., Synthesis, growth mechanism and thermal stability of copper nanoparticles encapsulated by multi-layer

graphene, Carbon 50 (6) (2012) 2119-2125.

[50]. Y. K. Chen, X. Zhang, E. Z. Liu, C. N. He, C. S. Shi, J. J. Li, et al., Fabrication of in-situ grown graphene reinforced Cu matrix composites, Sci. Rep. 6 (2016) 19363.

[51]. T. Babul, M. Baranowski, N. Sobczak, M. Homa, W. Leśniewski, Properties of Cu-matrix composites manufactured using Cu powder coated with graphene, J. Mater. Eng. Perform. 25 (8) (2016) 3146-3151.

[52]. H. Rho, S. Lee, S. Bae, T. Kim, D. S. Lee, H. J. Lee, et al., Three-dimensional porous copper-graphene heterostructures with durability and high heat dissipation performance, Sci. Rep. 5 (2015) 12710.

[53]. Y. K. Chen, X. Zhang, E. Z. Liu, C. N. He, Y. J. Han, Q. Y. Li, et al., Fabrication of three-dimensional graphene/Cu composite by in-situ CVD and its strengthening mechanism, J. Alloys Comp. 688 (2016) 69-76.

[54]. R.R. Nair, P. Blake, A. N. Grigorenko, K. S. Novoselov, T. J. Booth, T. Stauber, et al., Fine structure constant defines visual transparency of graphene, Science 320 (2008) 1308.

[55]. A. Siokou, F. Ravani, S. Karakalos, O. Frank, M. Kalbac, C. Galiotis, Surface refinement and electronic properties of graphene layers grown on copper substrate: an XPS, UPS and EELS study, Appl. Surf. Sci. 257 (23) (2011) 9785–9790.

[56]. T. Yoon, W. C. Shin, T. Y. Kim, J. H. Mun, T. -S. Kim, B. J. Cho, Direct measurement of adhesion energy of monolayer graphene as-grown on copper and its application to renewable transfer process, Nano Lett. 12 (3) (2012) 1448-1452.

[57]. J. Lahiri, T. S. Miller, A. J. Ross, L. Adamska, I. I. Oleynik, M. Batzill, Graphene growth and stability at nickel surfaces, New J. Phys. 13 (2011) 025001.

[58]. M. Vanin, J. J. Mortensen, A. K. Kelkkanen, J. M. Garcia-Lastra, K. S. Thygesen, K. W.

Jacobsen, Phys. Rev. B 81 (2010) 081408.

[59]. Y. X. Tang, X. M. Yang, R. R. Wang, M. X. Li, Enhancement of the mechanical properties of graphene–copper composites with graphene–nickel hybrids, Mater. Sci. Eng. A 599 (2014) 247-254.

[60]. F. Y. Chen, J. M. Ying, Y. F. Wang, S. Y. Du, Z. P. Liu, Q. Huang, Effects of graphene content on the microstructure and properties of copper matrix composites, Carbon 96 (2016) 836-842.

[61]. S. C. Tjong, Recent progress in the development and properties of novel metal matrix nanocomposites reinforced with carbon nanotubes and graphene nanosheets, Mater. Sci. Eng. R 74 (10) (2013) 281-350.

[62]. W. M. Daoush, B. K. Lim, C. B. Mo, D. H. Nam, S. H. Hong, Electrical and mechanical properties of carbon nanotube reinforced copper nanocomposites fabricated by electroless deposition process, Mater. Sci. Eng. A 513 (2009) 247-253.

[63]. K. T. Kim, S. I. Cha, S. H. Hong, S. H. Hong, Microstructures and tensile behavior of carbon nanotube reinforced Cu matrix nanocomposites, Mater. Sci. Eng. A 430 (1) (2006) 27-33.

[64]. S. I. Cha, K. T. Kim, S. N. Arshad, C. B. Mo, S. H. Hong, Extraordinary strengthening effect of carbon nanotubes in metal-matrix nanocomposites processed by molecular-level mixing, Adv. Mater. 17 (11) (2005) 1377-1381.

[65]. A. Brendel, V. Paffenholz, T. Köck, H. Bolt, Mechanical properties of SiC long fibre reinforced copper, J. Nuclear Mater. 386 (2009) 837-840.

[66]. J. H. Zhu, L. Liu, B. Shen, W. B. Hu, Mechanical properties of Cu/SiC_p composites fabricated by composite electroforming, Mater. Lett. 61 (13) (2009) 2804-2809.

[67]. Y. Z. Zhan, G. D. Zhang, The effect of interfacial modifying on the mechanical and wear properties of SiC_p/Cu composites, Mater. Lett. 57 (29) (2003) 4583-4591.

[68]. G. S. Wang, G. H. Fan, L. Geng, W. Hu, Y. D. Huang, Microstructure evolution and mechanical properties of TiB_2/Cu composites processed by equal channel angular pressing at elevated temperature, Mater. Sci. Eng. A 571 (2013) 144-149.

[69]. D. H. Kwon, T. D. Nguyen, K. X. Huynh, P. P. Choi, M. G. Chang, Y. J. Yuma, et al., Mechanical, electrical and wear properties of Cu-TiB_2 nanocomposites fabricated by MA-SHS and SPS, J. Ceram. Process. Res. 7 (3) (2006) 275-279.

[70]. ASM Handbooks, Properties and selection: nonferrous alloys and special purpose materials, ASM International, vol. 2, 1990, p. 3470.

[71]. J. Shuai, L.Q Xiong, L. Zhu, W.Z Li, Enhanced strength and excellent transport properties of a superaligned carbon nanotubes reinforced copper matrix laminar composite, Compos Part A: Appl Sci Manuf. 88 (2016) 148-155.

[72]. C. Arnaud, F. Lecouturier, D. Mesguich, N. Ferreira, G. Chevallier, C. Estournès, High strength–High conductivity double-walled carbon nanotube–Copper composite wires, Carbon 96 (2016) 212-215.

[73]. Y. Jin, L. Zhu, W. D. Xue, W. Z. Li, Fabrication of superaligned carbon nanotubes reinforced copper matrix laminar composite by electrodeposition, Trans. Nonferrous Met. Soc. China. 25 (9) (2015) 2994-3001.

[74]. R. R. Jiang, X. F. Zhou, Q. L. Fang, Z. P. Liu, Copper–graphene bulk composites with homogeneous graphene dispersion and enhanced mechanical properties, Mater. Sci. Eng. A 654 (2016) 124-130.

[75]. P. Yih, D. D. L. Chung, Silicon carbide whisker copper-matrix composites fabricated by

hot pressing copper coated whiskers, J. Mater. Sci. 31 (2) (1996) 399-406.

[76]. X. Luo, Y. Q. Yang, Y. C. Liu, Z. J. Ma, M. N. Yuan, Y. Chen, The fabrication and property of SiC fiber reinforced copper matrix composites, Mater. Sci. Eng. A 459 (1) (2007) 244-250.

[77]. Z. Y. Ma, S. C. Tjong, High temperature creep behavior of in-situ TiB_2 particulate reinforced copper-based composite, Mater. Sci. Eng. A 284 (1) (2000) 70-76.

[78]. P. Yih, D. D. L. Chung, Titanium diboride copper-matrix composites, J. Mater. Sci. 32 (7) (1997) 1703-1709.

[79]. L. Liu, Y. P. Tang , H. J. Zhao, J. H. Zhu, W. B. Hu, Fabrication and properties of short carbon fibers reinforced copper matrix composites, J. Mater Sci. 43 (3) (2008) 974-979.

[80]. Y. Z. Wan, Y. L. Wang, H. L. Luo, X. H. Dong, G. X. Cheng, Effects of fiber volume fraction, hot pressing parameters and alloying elements on tensile strength of carbon fiber reinforced copper matrix composite prepared by continuous three-step electrodeposition, Mater. Sci. Eng. A 288 (1) (2000) 26-33.

[81]. S.W. Chang, A.K. Nair, M.J. Buehler, Nanoindentation study of size effects in nickel–graphene nanocomposites, Phil. Mag. Lett. 93 (4) (2013) 196-203.

[82]. M. J. Hÿtch, E. Snoeck, R. Kilaas, Quantitative measurement of displacement and strain fields from HREM micrographs, Ultramicroscopy 74 (3) (1998) 131-146.

[83]. M. Estili, A. Kawasaki, Y. Pittini-Yamada, I. Utke, J. Michler, In situ characterization of tensile-bending load bearing ability of multi-walled carbon nanotubes in alumina-based nanocomposites, J. Mater. Chem. 21 (12) (2011) 4272-4278.

[84]. L. Gong, I. A. Kinloch, R. J. Young, I. Riaz, R. Jalil, K. S. Novoselov, Interfacial stress transfer in a graphene monolayer nanocomposite, Adv. Mater. 22 (2010) 2694-2697.

[85]. D.A. Mortimer, M. Nicholas, The wetting of carbon by copper and copper alloys, J. Mater. Sci. 5 (2) (1970) 149-155.

ACCEPTED MANUSCRIPT